Isolation and Characterization of Nontubular Sca-1$^+$Lin$^-$ Multipotent Stem/Progenitor Cells from Adult Mouse Kidney

Benjamin Dekel,* Lior Zangi,* Elias Shezen,* Shlomit Reich-Zeliger,*
Smadar Eventov-Friedman,* Helena Katchman,* Jasmin Jacob-Hirsch,[†] Ninette Amariglio,[†]
Gideon Rechavi,[†] Raanan Margalit,* and Yair Reisner*

*Department of Immunology, Weizmann Institute of Science, Rehovot, and [†]Department of Pediatric Hemato-Oncology and Functional Genomics, Sheba Medical Center, Tel-Hashomer, Israel

Tissue engineering and cell therapy approaches aim to take advantage of the repopulating ability and plasticity of multipotent stem cells to regenerate lost or diseased tissue. Recently, stage-specific embryonic kidney progenitor tissue was used to regenerate nephrons. Through fluorescence-activated cell sorting, microarray analysis, *in vitro* differentiation assays, mixed lymphocyte reaction, and a model of ischemic kidney injury, this study sought to identify and characterize multipotent organ stem/progenitor cells in the adult kidney. Herein is reported the existence of nontubular cells that express stem cell antigen-1 (Sca-1). This population of small cells includes a CD45-negative fraction that lacks hematopoietic stem cell and lineage markers and resides in the renal interstitial space. In addition, these cells are enriched for β1-integrin, are cytokeratin negative, and show minimal expression of surface markers that typically are found on bone marrow–derived mesenchymal stem cells. Global gene profiling reveals enrichment for many genes downstream of developmental signaling molecules and self-renewal pathways, such as TGF-β/bone morphogenic protein, Wnt, or fibroblast growth factor, as well as for those that are involved in specification of mesodermal lineages (myocyte enhancer factor 2A, YY1-associated factor 2, and filamin-β). *In vitro*, they are plastic adherent and slowly proliferating and result in inhibition of alloreactive CD8$^+$ T cells, indicative of an immune-privileged behavior. Furthermore, clonal-derived lines can be differentiated into myogenic, osteogenic, adipogenic, and neural lineages. Finally, when injected directly into the renal parenchyma, shortly after ischemic/reperfusion injury, renal Sca-1$^+$Lin$^-$ cells, derived from ROSA26 reporter mice, adopt a tubular phenotype and potentially could contribute to kidney repair. These data define a unique phenotype for adult kidney–derived cells, which have potential as stem cells and may contribute to the regeneration of injured kidneys.

Regenerative medicine is focused on the development of cells, tissues, and organs for the purpose of restoring function through transplantation (1). In this regard, the use of stem cells offers new and powerful strategies for future tissue development and engineering. Stem cells are defined by two major criteria: Pluripotentiality and self-renewal capacity. Perhaps the most characterized stem cell is one that resides in the adult bone marrow (BM), that is, the hematopoietic stem cell (HSC), which gives rise to all blood cell types (2). In addition, mesenchymal stem cells (MSC) are multipotent cells that can be isolated from adult BM and several other tissues and induced *in vitro* and *in vivo* to differentiate into a variety of mesenchymal tissues, including bone, cartilage, tendon, fat, BM

stroma, and muscle (3). Recently, it was suggested that BM-derived stem cells can cross boundaries and give rise to a broader array of differentiated cell types, that is, turning blood into liver, brain, pancreas, skin, intestine, and eventually kidney (4–11). However, this phenomenon remains controversial for several reasons. First, several studies cast doubt on the biologic significance and even the existence of such transdifferentiation (12,13). Second, some other investigations that do show a donor cell phenotype in parenchymal cells after transplantation of BM-derived stem cells suggest that it occurs through cell fusion and not by transdifferentiation and generation of cells *de novo* (14–16). Therefore, the term "regeneration" is used erroneously in this context and should be replaced by "reparative," if indeed that is shown to be the result of stem cell fusion. Third, whether by transdifferentiation or cell fusion, the efficiency of these processes under basal conditions and even when inflicting tissue injury is low, underscoring the functional capacity of adult BM-derived stem cells. For instance, in the kidney, several studies have shown that BM-derived cells adopt the phenotype of proximal tubular cells during acute tubular injury (10,11), as well as that of glomerular

endothelial and mesangial cells during glomerular injury (17–19), but only a few report on mild improvement in kidney function (10).

These obstacles emphasize the need to seek renal progenitor cells beyond the few known extrarenal sources. Recent studies have attempted to isolate and characterize tissue stem cells by identifying organ cells that display specific stem cell phenotypes. One such strategy is to identify organ cells that express stem cell antigens (20–23). Of interest are those that were used previously to define murine BM-derived hematopoietic stem cells, primarily stem cell antigen-1 (Sca-1), c-kit, and CD34 (2). Sca-1 is a member of the Ly-6 family and first was reported as one of the early cell surface markers of hematopoietic stem cells (2). Recent reports have demonstrated that multipotential stem cells that were derived from BM and skeletal muscle express Sca-1 (3,21,22,24,25). Moreover, it was shown recently that beyond its role as a marker for muscle progenitors, Sca-1 has an active function in myogenesis (26). Nevertheless, this approach might be complicated by the presence of Sca-1 on mature cells, as shown for medullary renal tubular epithelium and pulmonary vascular endothelium (27,28).

Recently, we showed that early embryonic human and porcine renal precursors remarkably can grow, differentiate, and undergo vascularization, achieving successful organogenesis of urine-producing miniature kidneys (29). It is interesting that cells that reside in these embryonic progenitor tissues exhibit the potential to differentiate, after transplantation or *in vitro* manipulation, into other professional cell types, in addition to renal epithelia, that participate in kidney organogenesis (myofibroblasts, smooth muscle, and endothelium), as well as nonrenal derivatives, including cartilage, bone, and blood (29–32). These studies suggested the presence of multipotent embryonic renal stem cells. Unfortunately, although highly proliferative, they can be used only in the allogeneic setting, whereas adult cells represent an autologous source.

Here we identified a population of nontubular Sca-1$^+$Lin$^-$ cells in the adult kidney, which are distinct from HSC and their progeny. Additional *in vitro* and *in vivo* studies suggest that the cells of this fraction are putative kidney-derived stem cells.

Materials and Methods
Animals
The mice used were 8 to 12 wk of age. C57BL/6, SJL, CB6F1, and ROSA26 mice were obtained from the Weizmann Institute Animal Center (Rehovot, Israel). DBA/2 mice were obtained from the Roscoe B. Jackson Memorial Laboratory (Bar Harbor, ME). A breeding pair of transgenic H-2^b mice that expressed the T cell receptor (TCR) from the CTL clone 2C with specificity for H-2L^d was provided by J. Nikolic-Zugic (Sloan-Kettering Institute, New York, NY). All protocols were approved by the Institutional Animal Care and Use Committee of the Weizmann Institute of Science.

Isolation and Characterization of Sca-1$^+$ Cells from the Adult Murine Kidney
Kidneys of adult (10- to 12-wk-old) C57BL/6 mice were washed extensively with sterile PBS to remove contaminating debris and red blood cells (RBC). Kidneys then were diced and treated with 0.075% collagenase (type D; Sigma-Aldrich, St. Louis, MO) diluted in PBS for 10 min at 37°C with gentle agitation. The collagenase was inactivated with an equal volume of culture medium (DMEM/10% FCS/1% penicillin streptomycin), and the dissolved tissue was minced further and centrifuged for 10 min at low speed. The cellular pellet was resuspended in culture medium and sequentially filtered through 70- and 40-μm mesh filters to remove debris and cell segments. Cell suspensions were treated with cold ACK buffer (0.15 M potassium-ammonium chloride buffer) to remove remaining RBC. A comparison of kidney cells, obtained through mincing and filtration, with or without collagenase, yielded similar results.

Enrichment of Sca-1$^+$ cells was achieved by incubating cells with anti–Sca-1 microbeads (Miltenyi Biotec, Auburn, CA) and purification by at least two cycles of magnetic selection (20). Sorted populations were reanalyzed by flow cytometry, and the purity of Sca-1$^+$ cells was confirmed before use. FACS analysis was performed using a modified FACScan (BD Biosciences, Mountain View, CA). Fluorescence data were collected using three-decade logarithmic amplification on 25 to 50×10^3 viable cells, as determined by forward light scatter intensity. Cells were labeled with Sca-1-PE, Sca-1-APC, Sca-1-Biotin; CD45-, B220-, Mac-1 (CD11b)-, NK-, TER119-, CD11c-, CD29-, I-AD-, Fas (CD95)-, and H-2^b-FITC (BD Pharmingen, San Diego, CA); CD34-, CD31-, CD25-, Gr-1-, CXCR4-, CD62L-, CD49e-, CD44-, CD90-, Flk-1-, EpCAM- (all Pharmingen), and c-Kit-PE (SBA, Birmingham, AL); CD4- and CD8-PerCp (Pharmingen). Biotinylated B7.1 (CD80), B7.2 (CD86; SBA), and 1B2 antibodies (provided by J. Nikolic-Zugic, Sloan-Kettering Institute) were detected with streptavidin-PerCp or streptavidin-APC (Jackson ImmunoResearch Laboratories, West Grove, PA), and nonviable cells were detected with propidium iodide (PI). PE-rat IgG2a, FITC-hamster IgG (Serotec, Oxford, UK), and PerCp- and APC-streptavidin were used as controls. FACS sorting was performed using BD FACSAria, a high-speed sorter (acquisition rates of up to 70,000 events/s) with fixed-alignment cuvette flow cell and up to three air-cooled lasers at 488-, 633-, and 407-nm wavelengths. Cells were sorted in a cold and sterile environment for high and low PE staining (Sca-1). Sca-1^{bright} and Sca-1^{dim} cells were collected into different cold glass FACS tubes, and after cells were centrifuged, they were transferred to culture medium and incubated at 37°C, 7% CO_2 on plastic plates.

Immunohistochemistry
Cryostat and paraffin sections, cells growing on plastic, and glass smears of renal Sca-1$^+$ cell preparations were immunoperoxidase labeled and specified antibodies and secondary reagent system, DAKO Envision + System, HRP (DAKO, Glostrup, Denmark), were applied using DAB as chromogen. Nuclei were counterstained by hematoxylin. The following antibodies were applied: Polyclonal rabbit anti-cytokeratin (wide-spectrum screening), polyclonal rabbit anti-cow S-100, mouse monoclonal anti-neurofilament (NF), and mouse monoclonal anti-α-smooth muscle actin (all from DAKO); rat monoclonal anti-F4/80 (Serotec); rat monoclonal anti-CD31 (Chemicon Hampshire, UK); rat monoclonal anti–Sca-1 (BD Pharmingen); mouse monoclonal anti-vimentin (Clone VIM-13.2) and rabbit anti-laminin (both from Sigma); rabbit anti-β-galactosidase (Abcam, Cambridge, MA; 1:2000, overnight incubation); and mouse monoclonal anti-CD45 (clone 2B11 + PD7/26; Dako). For immunofluorescent labeling, acetone-fixed sections of adult mouse kidney (6 μm) were incubated with a mixture of polyclonal rabbit anti–von Willebrand factor, polyclonal rabbit anti-cytokeratin (Dako), and rat anti–Sca-1 (BD Pharmingen). Nuclei were counterstained with Hoechst33342. The following secondary antibodies were applied: Texas Red–conjugated donkey anti-mouse antibody and Cy2-conjugated goat anti-rabbit antibody (both from Jackson ImmunoResearch Laboratories). Paraformaldehyde-fixed cultures were labeled with mouse anti-human nestin (CRP, Cumberland, VA) and rabbit

anti-mouse β-tubulin III (CRP) followed by incubation with donkey anti-mouse or anti-rabbit Cy3-conjugated secondary antibodies (Jackson). For all immunohistochemical stainings, a negative control was run using the same technique but omitting the primary antibody while adding the labeled secondary antibody.

Cell Culture

Renal Sca-1$^+$Lin$^-$ cells were incubated at 37°C, 7% CO$_2$ on plastic plates in culture with DMEM 1.0 g/ml glucose + 10% FCS + 1% penicillin streptomycin (Biological Industries, BetHaemek, Israel). After 7 d in culture, an enriched population of Sca-1$^+$Lin$^-$ cells was plated. Cultures were maintained with medium that was exchanged every 2 to 3 d, and transfers were done when needed. For establishment of single-cell clones, isolated Sca-1$^+$Lin$^-$ cells were suspended in 10 ml of culture medium. Cells were counted and diluted to reach an average of 1 cell/200 μl culture medium and replated into 96-well culture plates (200 μl/well), as described previously (25).

Estimation of Multipotency

For enhancement of differentiation of freshly isolated and cloned renal Sca-1$^+$Lin$^-$ cells into several cells type, 10^5 intact cells were plated. Osteogenic differentiation was induced in culture medium, 50 μg/ml ascorbic acid, 10 mM β-glycerophosphate, and 10^{-8} M dexamethasone. Cell differentiation was tested 3 wk later. For detection of osteocytes, alizarin red staining (Sigma) and nitro blue tetrazolium staining (DAKO) for alkaline phosphatase were used as described previously (25). For enhancement of adipocyte differentiation, culture medium was supplemented with 1-methyl-3-isobutylxanthine, 10^{-9} M dexamethasone, 5 mM insulin, and 5 mM indomethacin (Stemcell Technologies, Vancouver, BC, Canada). For detection of oil droplets, cultures were stained in saturated Oil-Red O solution (Sigma) in 60% isopropanol (25).

Neural differentiation was induced by supplementing the culture medium with human basic fibroblast growth factor (FGF; 100 ng/ml) during the first week of culture followed by FGF-8b (10 ng/ml) and brain-derived neurotrophic factor (10 ng/ml) during the second and third weeks, respectively. Neural differentiation was assessed by specific morphology and expression of nestin and β-tubulin III (see above).

Array Processing

All experiments were performed using Affymetrix Mouse 430A2.0 oligonucleotide arrays, as described at http://www.affymetrix.com/support/technical/datasheets/rat230_2_datasheet.pdfURL1. Total RNA from each sample pool was used to prepare biotinylated target RNA, with minor modifications from the manufacturers recommendations (http://www.affymetrix.com/support/technical/manual/expression_manual.affx). Details of quality control measures can be found at http://eng.sheba.co.il/genomics.

Array Analysis

The hybridization results were analyzed using MAS 5. Probe sets with signals lower than 20 were filtered out. The t test was applied as a probability measure ($P < 0.05$) of Sca-1$^+$ and Sca-1$^-$ discrimination samples with $P < 0.05$ further filtered using a signal average 1.5-fold change threshold. Probe sets that were up- or downregulated by at least 1.5-fold were classified into functional groups using Go Annotation tools (Dennis G Jr *et al.*, DAVID: Database for Annotation, Visualization, and Integrated Discovery, http://apps1.niaid.nih.gov/David/upload.asp).

Assay for Inhibition of Immune Stimulation in the 2C TCR Transgenic Mouse Model

Spleen cells of 2C transgenic H-2^b mice, expressing the TCR-$\alpha\beta$ with specificity for H-2L^d mice, were harvested, and cell suspensions were treated with Tris-buffered ammonium chloride to remove RBC and brought to a concentration of 2 × 10^6 cells/ml in RPMI 1640 complete tissue culture medium at 37°C in a 5% CO$_2$/air incubator. The cells (2 × 10^6/ml) then were stimulated with irradiated (20 Gy) DBA/2 splenocytes (2 × 10^6/ml) in the presence or the absence of 10, 5, 1, and 0.5% cells of specific (DBA/2 origin) and nonspecific (SJL origin) newly isolated and cultured renal Sca-1$^+$ cells and BM-derived MSC. Cultures were incubated for 72 h in 24-well plates. The inhibition of proliferation of specific effector T cells was monitored by cytofluorimetric analysis, measuring the level of 2C transgenic cells, specifically stained by the 1B2 antibody, directed against the clonotypic anti–H-2L^d TCR.

Ischemia/Reperfusion Injury and Cell Transfer

Ischemia/reperfusion (I/R) injury was performed by occluding the left renal pedicle for 30 min (11). A volume of 50 μl of cell suspension that contained newly isolated Sca-1$^+$ cells from ROSA26 was injected directly into the left kidney through the renal pelvis with a 32-G needle shortly after removal of the vascular clamp. The needle was advanced into the renal parenchyma, and the cell suspension was injected slowly. For controls, (1) mice were subjected to an identical protocol of I/R but received PBS or Sca-1$^-$ cells instead of Sca-1$^+$ cells or (2) received the same amounts of cells without bearing ischemic injury.

Results
Progenitor Cells in the Adult Mouse Kidney

Taking into account that Sca-1 is expressed on renal parenchymal cells, mostly distal tubules in the cortex and medullary cords (27), we aimed to isolate a "tubular-depleted" fraction of kidney cells initially using mild digestion, which predominantly affects loosely bound cells and not those that are integrated within tight junctions, followed by gentle mechanical mincing and sequential filtration through a 70- and 40-μ mesh to deplete large cells and undigested tubular segments and tissue fragments. RBC were depleted with the addition of ACK (see Materials and Methods). This cell preparation does not represent all of the cells that are present in the adult kidney. The cell suspensions were co-stained with both PE-labeled anti–Sca-1 and FITC-labeled anti-CD45 to determine cells of hematopoietic origin. For control, the same method was applied to mouse spleen. Typical results of dual-wavelength FACS are shown in Figure 1. As can be seen in Figure 1, A and B, a distinct population in both spleen and kidney can be observed on the forward (FSC) and sidescatter (SSC) plot ("lymphogate"). Analysis of CD45 expression in the spleen within this gate reveals a predominant CD45$^+$ cell population of hematopoietic origin, with the highest proportion of Sca-1$^-$CD45$^+$ cells (tissue leukocytes) and to a much lesser extent Sca-1$^+$CD45$^+$ cells (Figure 1C). In the kidney preparation, we also could observe a CD45$^-$ fraction that expresses the Sca-1 marker (Sca-1$^+$CD45$^-$ cells, representing 0.5 to 1% of the total cell suspension; Figure 1D). The finding that spleen cells, prepared under identical conditions, were devoid of this CD45$^-$ fraction indicated that it was not an artifact resulting from loss of this surface marker during preparation of cell suspensions. It I interesting that as the size of the gate increased and contained
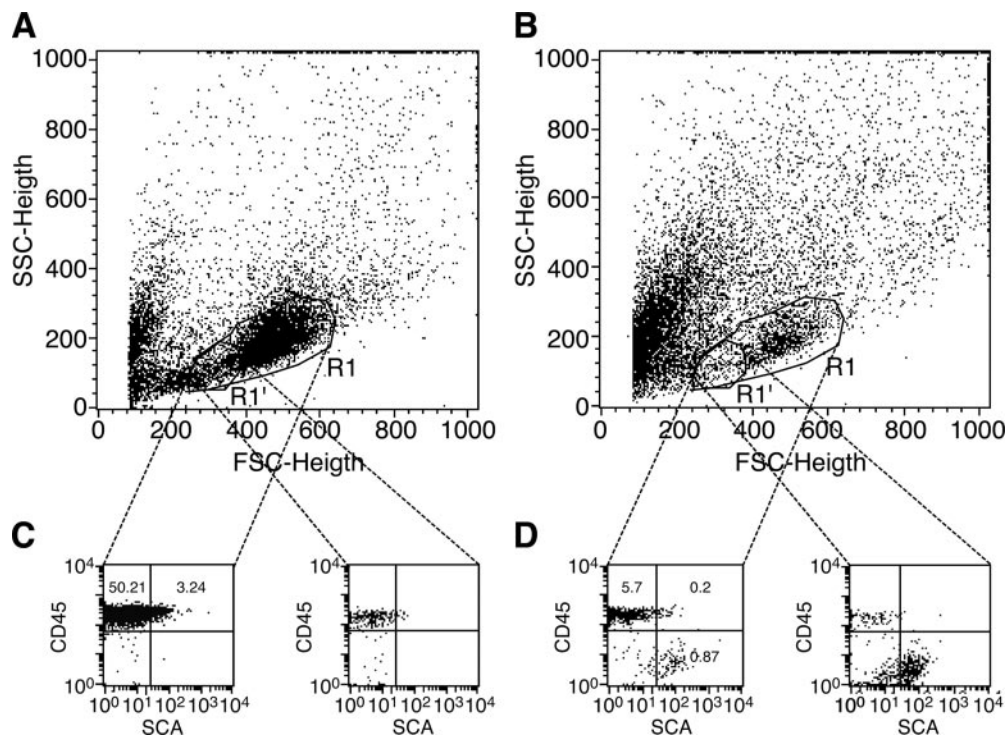
Figure 1. Identification of stem cell antigen-1–positive (Sca-1$^+$)CD45$^-$ cells in adult mouse kidney. (A and B) FACS analysis of adult spleen (A) and kidney (B) cells: Representative forward (FSC) and side (SSC) scatter plot. Boxed cells in R1 represent the lymphogate in spleen and kidney, whereas R1′ represents cells with smaller size in the lymphogate. (C and D) Spleen and kidney cells were stained further with Sca-1 and CD45 antibodies to distinguish cells of hematopoietic origin. A Sca-1$^+$CD45$^-$ cell fraction is observed in the kidney within R1 and R1′ (D).

smaller cells (according to the FSC), the Sca-1$^+$CD45$^-$ cell fraction increased. Moreover, exclusively gating the smaller cells (R1′) revealed a more predominant Sca-1$^+$CD45$^-$ cell population at the expense of the Sca-1$^-$CD45$^+$ phenotype (Figure 1D). When preparing cells without ACK to include RBC and staining for the erythrocyte antigen Ter119, we could show that although the majority of cells within the R1′ gate are Ter119$^+$Sca-1$^-$, a population of Sca-1$^+$Ter119$^-$ cells still exists (data not shown). Thus, within the kidney lymphogate, the cell preparation can be separated into CD45$^+$ and CD45$^-$ cells. We hypothesized that the Sca-1$^+$CD45$^-$ fraction contained renal-derived progenitor cells.

In Situ *Detection of Sca-1$^+$Lin$^-$ Cells in the Adult Kidney*

Identification of renal Sca-1$^+$CD45$^-$ cells in the FACS within the lymphogate suggested a nontubular origin of the cells. Moreover, because the number of Sca-1$^+$CD45$^+$ cells is negligible (see above), immunostaining of Sca-1 could detect such cells *in situ*. We therefore performed Sca-1 immunohistochemistry on frozen sections of adult murine kidneys (Figures 2 and 3). As has been reported (27), we found intense Sca-1 staining in the medullary cords, as well as linear Sca-1 immunostaining in a pattern that was consistent with expression in endothelial cells of large and small renal arteries (Figure 2, A and B). Sca-1 expression was not detected by immunostaining in capillaries. Striking, we also could show intense and diffuse staining in the renal papilla (Figure 2, C and D). To delineate further the

presence of Sca-1$^+$ cells in the papillary region, we used double immunofluorescence for cytokeratin and Sca-1 with nuclear counterstaining (Hoechest33342). Whereas renal tubular cells, which express both Sca-1 (red) and CK (green) appear in yellowish color (Figure 2E), cells that are labeled in red indicate nontubular Sca-1$^+$ cells. These cells can be found in the very outer part of the papilla (Figure 2F) and in close proximity to tubules, some of which are adjacent to the tubular basal surface (Figure 2, G through J). Nontubular Sca-1–expressing cells also could be found in the cortex and medulla but to a much lesser extent (Figure 3). Here, double immunofluorescence for Sca-1 (green) and von Willebrand factor (a marker of endothelial cells, red) demonstrated mostly tubular Sca-1 staining but also scarce Sca-1$^+$ cells in the interstitial space outside vessels. Thus, in accordance with the FACS data, immunostaining identified a population of nontubular Sca-1$^+$ cells, mostly in the renal papilla.

Enrichment and Characterization of Nontubular Sca-1$^+$ Cells

Because our initial kidney cell preparation enriches the presence of fractions of cells within the lymphogate, we used anti–Sca-1 microbeads and the MACS system for further enrichment of renal Sca-1$^+$ cells within that population. This takes advantage of the lack of CD45$^+$ Sca-1$^+$ cells in the naïve kidney and depletes the major population of CD45$^+$ Sca-1$^-$ cell tissue lymphocytes but can result in the contamination of mature
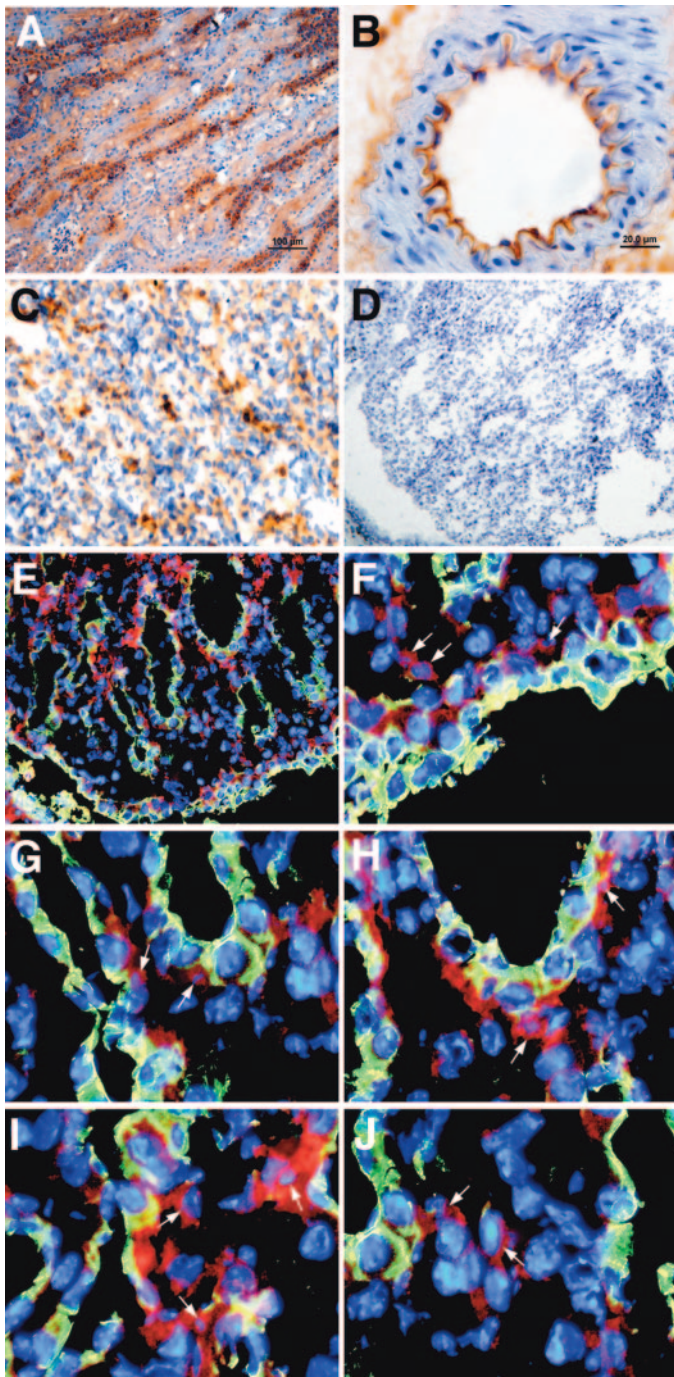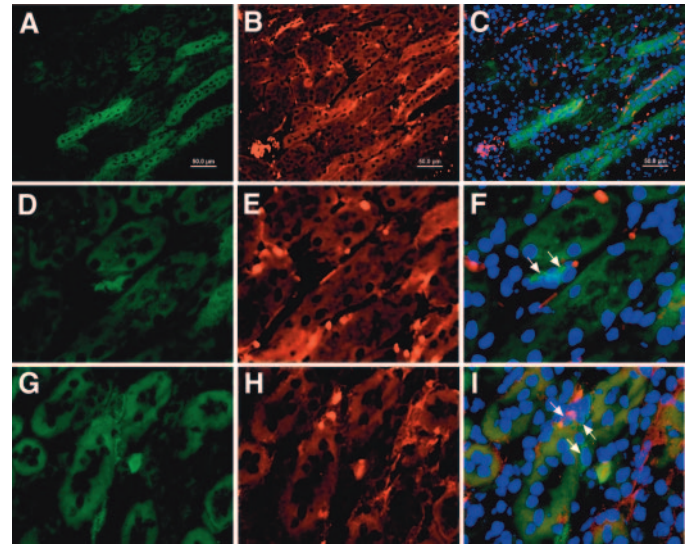
Figure 3. In situ detection of nontubular renal Sca-1$^+$ cells in medulla and cortex. Double immunofluorescence was performed to detect Sca-1 expression (tubular and nontubular; green, A, D, and G) and von Willebrand factor (vWF), which stains endothelial cells (red; B, E, and H) in medullary sections. Overlaid images are shown in (C, F, and I). Lower magnification (A through C) and higher magnification (D through F) of the same field, as well higher magnification of a different field, all showing nontubular Sca-1 cells (arrows). Magnifications: ×40 in A through C; ×100 in D through F.

Figure 2. In situ detection of nontubular renal Sca-1$^+$ cells in papilla. Frozen sections of adult kidney were immunostained with anti-mouse Sca-1. Shown is positive staining in medullary cords (A) and small arteriole (B). Diffuse staining was observed in the renal papilla (C), whereas control staining of the papilla without primary antibody was negative (D). (E and F) Double immunofluorescence was performed to detect Sca-1 expression (red) and cytokeratin (green). Images were overlaid to demonstrate co-localization of Sca-1 and CK (yellow). (E) Renal papilla. (F) Outer part of the papilla; nontubular Sca-1 cells are indicated in red (G through J) Several high-magnification fields of the papilla showing nontubular Sca-1 cells (red, arrows) in close proximity and adjacent to tubular cells (yellow). Magnifications: ×10 in A, C, and D; ×100 in B and F through J; ×40 in E.

epithelial Sca-1$^+$ cells. A representative SSC/FSC plot is shown after this step (Figure 4A). FACS analysis revealed that Sca-1$^+$ cells were enriched to >90% when kidney cell suspension was sorted twice with the MACS system, with <0.5% of Sca-1$^+$ cells in the negative fraction (Figure 4B). Moreover, analysis of CD45 and Sca-1 expression within the lymphogate (R1) revealed that the Sca-1$^+$CD45$^-$ cell population was enriched to approximately 6 to 10% of the total population (Figure 4B).

To analyze further the enriched Sca-1$^+$ cell population, we sorted different subpopulations by flow cytometry according to the size and granularity (R1 through R3), and these were cytospun for immunohistochemical characterization (Figure 4, C and D). Here we identified R2 as a large population of cell fragments (approximately 50% of the total population, mostly cytoplasms devoid of nuclei) and R3 (the highly granular and scattered cell fraction) to be composed of cell fragments but also epithelial cell aggregates positive for cytokeratin (Figure 4D). Both R2 and R3 are strongly positive for Sca-1 in both FACS and immunostaining and could result in overestimation of Sca-1$^+$ cells, if included in the analysis. It is interesting that a close histologic examination of the sorted R1 lymphogate fraction revealed two subpopulations that could not be discriminated by the sorting method and indicated that it is not entirely a pure population. Indeed, immunostaining of the R1 population demonstrated differential staining for Sca-1, with the smaller cells intensely expressing Sca-1 and the larger ones only low levels of staining (Figure 4C). In addition, the R1 population was shown to express vimentin uniformly, confirmed to be
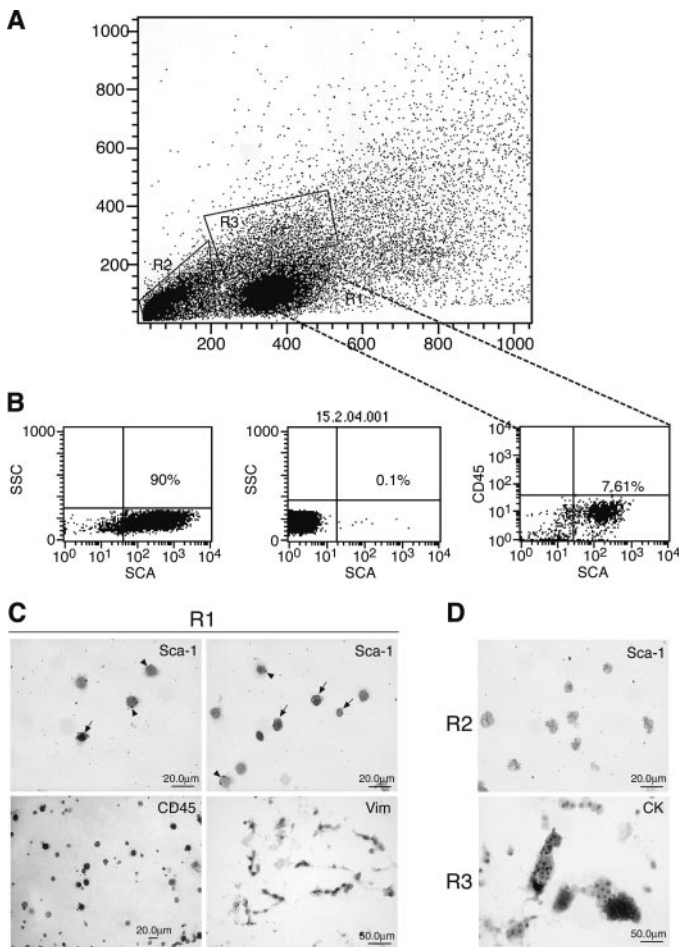
Figure 4. Isolation of nontubular renal Sca-1$^+$ cells. Sca-1$^+$ cells were enriched by the MACS system with anti–Sca-1 microbeads. (A) Representative FSC and SSC plot of the enriched cells, which is separated into three boxed areas (the lymphogate R1, as well as R2 and R3). (B) After sorting at least twice, approximately 90% of the cells expressed Sca-1, whereas the negative fraction contained <1% of Sca-1$^+$ cells. Cells that were stained with Sca-1 and CD45 antibodies demonstrate approximately 10-fold enrichment in the R1 Sca-1$^+$CD45$^-$ cell fraction. (C and D) The R1 through R3 fractions were analyzed further by cell sorting and immunostaining of sorted cells for Sca-1, CD45, vimentin, and pancytokeratin (CK). (C) R1 cells in the upper panels show differential expression of Sca-1 (intense staining in smaller cells [arrows] and patchy staining in larger cells [arrowheads]), whereas R1 cells in lower panels positively stain for vimentin and fail to stain CD45. (D) R2 sorted fraction is shown to be composed of cell fragments that are cells that are strongly positive for Sca-1, whereas tubular segments that express CK are found in R3. Magnification, ×100.

CD45$^-$ (Figure 4C), and failed to stain other differentiation markers, pan-cytokeratin, CD31 (endothelial), NF, S-100 (neuronal and neuroendocrine), and α-smooth muscle actin (smooth muscle; data not shown). Our isolation method yielded approximately 0.5×10^6 of these cells per four male kidneys. Further characterization of the R1 gated Sca-1$^+$ cells by FACS revealed that they lacked blood cell lineage markers (CD4, CD8, B220,

NK [CD56], Gr-1, Mac-1 [CD11b], CD11c, and TER119), as well as c-Kit, CD34, and FLK1 (Figure 5A, Table 1). These features argue against a hematopoietic progenitor cell. Analysis for mesenchymal, endothelial, and epithelial cell markers revealed that the Sca-1$^+$ cells were positive for CD29 (integrin-β1) but lacked CD44, CD49e, CD90, CD62L, CD31, and EpCAM (expression levels all were below isotype control), suggesting a distinct phenotype from BM-derived MSC (CD44$^+$CD49e$^+$CD62L$^+$), endothelial progenitor cells (FLK1$^+$CD31$^+$), and mature epithelial cells (EpCAM$^+$). It is interesting that Sca-1$^+$ cells showed very low expression levels of strain-specific MHC class I (H-2) and, failed to express MHC class II, co-stimulatory molecules CD80 (B7–1) and CD86 (B7–2), and IL-2 receptor (CD25; Figure 5B, Table 1).
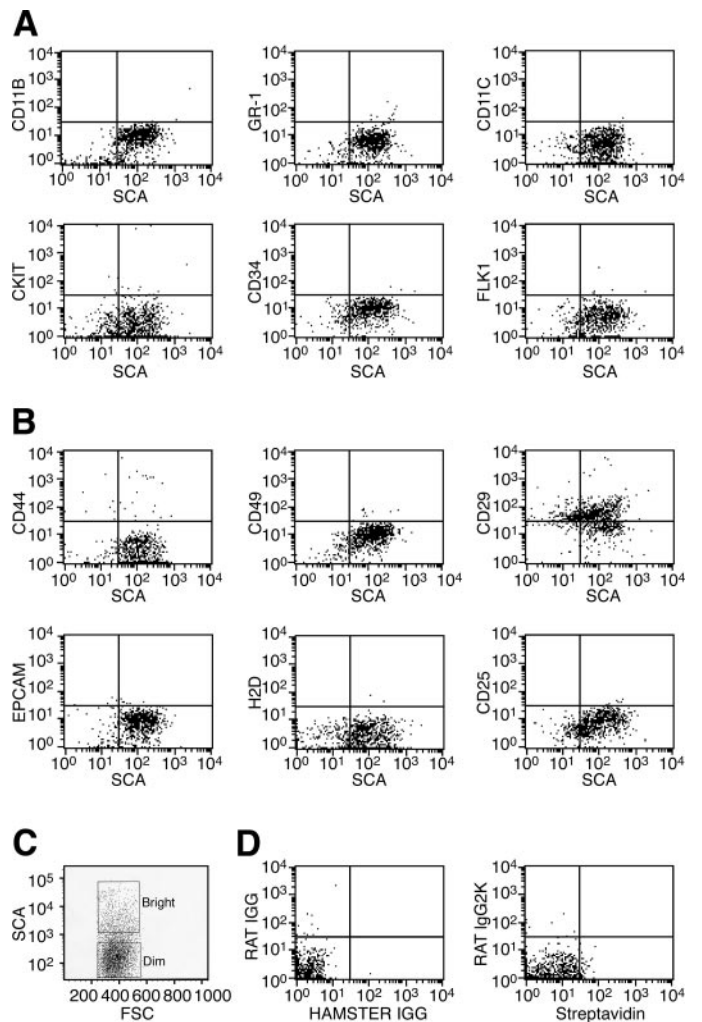

Figure 5. Flow cytometric analysis of nontubular Sca-1$^+$ cells. Enriched Sca-1$^+$ cells were labeled with Sca-1 plus the indicated (A) hematopoietic lineage (upper row) and progenitor cell markers (lower row) and (B) mesenchymal (upper row), epithelial, and immunologic markers (lower row). Double staining by FACS shows the frequency of Sca-1 and the various CD markers. In all samples, cells are gated in R1. (C) R1 sorted cells were stained with Sca-1 antibody and further sorted into Sca-1^{bright} and Sca-1^{dim} cells. (D) Isotype and streptavidin control staining.

Table 1. Immunophenotype of nontubular renal Sca-1^{+} cells[a]

Common Name	CD	Detection
Hematopoietic antigens		
CD3 complex	CD3e	Negative
T4 cell	CD4	Negative
T8 cell	CD8	Negative
B cell antigen	CD19	Negative
mucosialin	CD34	Negative
leukocyte common antigen	CD45	Negative
	CD45/B220	Negative
NK cell antigen	NK1.1	Negative
erythroid antigen	TER119	Negative
granulocyte antigen	Ly-6G	Negative
Thy-1	CD90	Negative
stem cell antigen	SCA-1	Positive
Adhesion molecules		
L-selectin	CD62L	Negative
E-selectin	CD62E	Negative
PECAM-1	CD31	Negative
HCAM	CD44	Negative
Integrins		
Mac1	CD11b	Negative
CR4 α chain	CD11c	Negative
VLA-5	CD49e	Negative
VLA-β1 chain	CD29	Positive
cytokine receptors		
IL-2R	CD25	Negative
c-Kit	CD117	Negative
Flk-1 (VEGF receptor-2)		Negative
Others		
B7.1	CD80	Negative
B7.2	CD86	Negative
MHC I	H-2K[b]	Negative
MHC II	I-Ag[7]	Negative

[a]Renal Sca-1^{+} cells were analyzed by FACS with a panel of antibodies using isotype controls to set up the initial gates. HCAM, homing-associated cell adhesion molecule; NK, natural killer; PECAM, platelet-endothelial cell adhesion molecule; Sca-1, stem cell antigen-1; VEGF, vascular endothelial growth factor; VLA, very late antigen.

Having established that the nontubular R1 fraction differentially expresses Sca-1 by immunostaining, we further sorted Sca-1^{bright} (signal intensity >10[3]) and Sca-1^{dim} (<10[3]) subpopulations, which are detected at a ratio of 1:10 cells, indicating the rarity of the R1 Sca-1^{bright} population (Figure 5C). Thus, magnetic bead sorting yields a fraction that is significantly enriched for nontubular Sca-1^{+}Lin^{−}CD45^{−} cells, and additional FACS sorting *via* specific gates increases its purity.

Culture and Cloning of Renal Sca-1^{+}Lin^{−} Cells

An enriched nontubular Sca-1^{+} cell fraction was isolated from adult murine kidneys by magnetic beads and cultured with enriched medium that contained FCS (see Materials and Methods). At culturing, renal Sca-1^{+} cells are floating cells, whereas within 24 to 72 h, a fraction of cells adhere to the culture dish and the remaining nonattached fraction consists of contaminating tubular segments, floating cell aggregates, and round cells (Figure 6A). Thus, renal tubular segments are discarded after short-term culture by continuous removal of the nonadherent fraction. Within 7 d, the Sca-1 culture consists of an adherent population of small round cells, whereas spindle-like and elongated shapes start to appear and increase with time (Figure 6, B and C). Flow cytometric analysis of trypsinized adherent cells 14 d in culture revealed decreased Sca-1 levels compared with fresh Sca-1^{+} cells; nevertheless, the former maintained a stable Sca-1^{+}Lin^{−}CD45^{−} phenotype (of the Lin analysis, only CD11b is shown). Moreover, cells typically failed to stain for c-Kit and CD44 (Figure 6D). Immunostaining on culture dishes revealed positive Sca-1 staining and weak immunoreactivity to α-smooth muscle actin (Figure 6, E and F, respectively), whereas pan-cytokeratin, CD31, NF, and S-100 were negative (data not shown).

It is interesting that culturing of the further sorted nontubular R1 Sca-1^{bright} cells showed that they are highly adherent (all of these cells adhere within 24 h with no apparent nonadherent cells) and transform into fibroblast-like cells (Figure 6, G and H). In contrast, The R1 Sca-1^{dim} cells represent a population that does not adhere and remains round cells (Figure 6I). Furthermore, double immunofluorescence of the Sca-1^{bright} cells, which start to appear as elongated cells, demonstrated intense vimentin expression and lack of CK staining (Figure 6, J through L). Thus, culturing of the highly purified R1 Sca-1^{bright} cells omits contaminating tubular and nonadherent cells in advance, promotes attachment, and yields similar results to the culture of the MACS Sca-1 cells.

To determine further the pluripotency of nontubular Sca-1^{+}Lin^{−} cells, we tested their capacity to differentiate into various types of cells after induction. For elimination of the possibility that the Sca-1^{+} cell population contains several progenitors that give rise to the different cell types, it is important to perform this analysis at the single-cell level. We therefore established clones of renal Sca-1^{+}Lin^{−} cells using standard single-cell cloning methods. In some experiments, after 10 d in culture to let cells adhere and elimination of the nonadherent fraction, single small round cells were isolated by limiting dilution into 96-well plates. Initially, these cells were quiescent, but they slowly started to proliferate, so by 4 wk, small clones of dispersed cells were formed, whereas by 8 wk, we observed cell aggregates that resembled neurospheres, previously identified in cultures of neuronal and skin stem cells (25) (Figure 7, A and B). After 10 wk, the clones were dissociated and moved to 24-well plates and then into 12-well plates over a period of 3 wk and subsequently into small flasks. Three independent clones of renal Sca-1^{+} cells were established. To date, the clonal isolates have been grown in culture for more than 12 passages with a doubling time of approximately 36 h. Immunocytochemical analysis of a representative cell clone revealed uniform expression of vimentin and laminin but not cytokeratin (Figure 7, C and D), whereas some cells were detectably positive for α-smooth muscle actin and others showed a migratory appear-
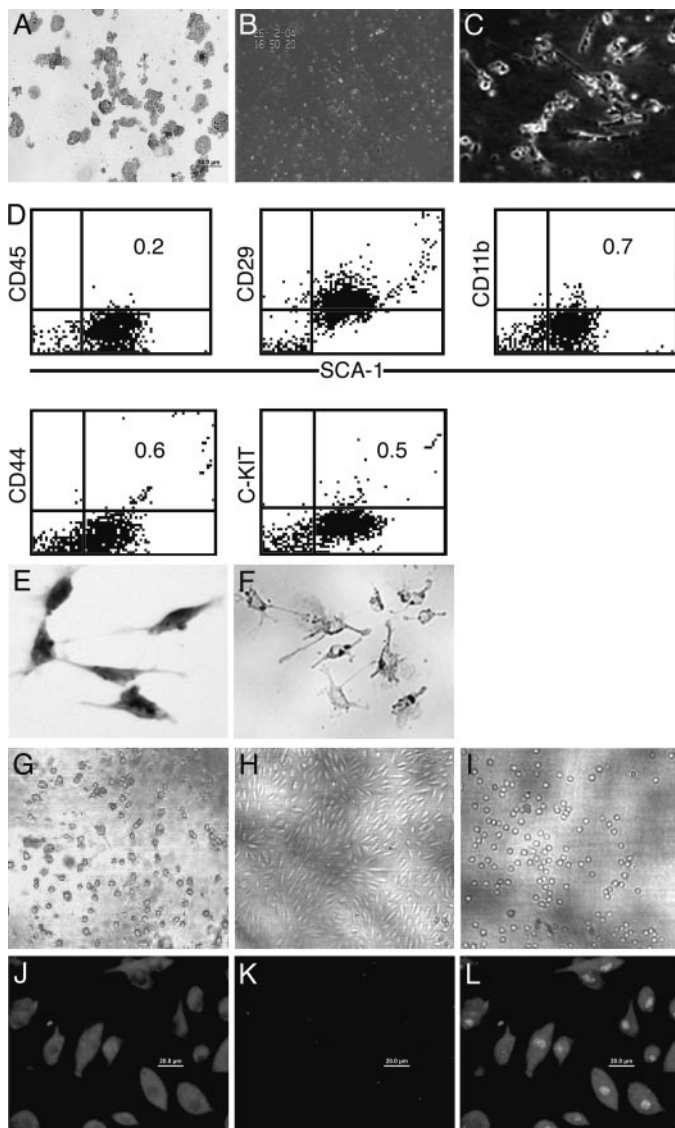
Figure 6. Cultured renal Sca-1$^+$Lin$^-$ cells. (A through E) Culture of enriched nontubular Sca-1$^+$ cell fraction after MACS. (A) Nonadherent fraction showing cell aggregates that positively immunostained for CK. (B and C) Phase contrast images of adherent fraction at 7 d in low (B) and higher (C) magnification, showing the appearance of spindle-like and elongated cells. (D) Flow cytometric analysis of trypsinized cells after 14 d in culture. Double staining by FACS shows the frequency of Sca-1 and the surface markers CD45, CD29, CD11b, CD44, and c-Kit. Immunostaining of elongated cells for Sca-1 (E) and α-smooth muscle actin (F). (G through I) Culture of FACS-sorted subpopulations. Phase contrast images of adherent nontubular R1 Sca-1^{bright} cells at 24 h (G) and 28 d (H) and nonadherent nontubular R1 Sca-1^{dim} cells, which remain round cells and are not viable (I). (J through L) Double immunofluorescence of cultured R1 Sca-1^{bright} cells for vimentin (red; J), cytokeratin (green; K), and overlaid image with nuclear counterstaining (Hoechst 33342; L). Magnifications: ×40 in A, E, and F; ×100 in J through L.

Figure 7. Characterization of cloned renal Sca-1$^+$Lin$^-$ cells. Clonal-derived cells demonstrate the formation of spheres (A, arrows, and B). Immunostaining of cloned cells shows positive staining for vimentin (C) and lack of staining for CK (D). Some cells were detectably positive for α-smooth muscle actin (E) and CD31 (G and H). Under nonconfluent conditions, a migratory dendritic-like phenotype can be observed (hematoxylin staining). Magnifications: ×10 in A, C, D, and G; ×40 in B; ×100 in E and H.

ance when nonconfluent (Figure 7, E and F). It is interesting that we found heterogeneous cell populations expressing CD31, a marker of endothelial cells (Figure 7, G and H). We then examined whether these cells could differentiate into os-
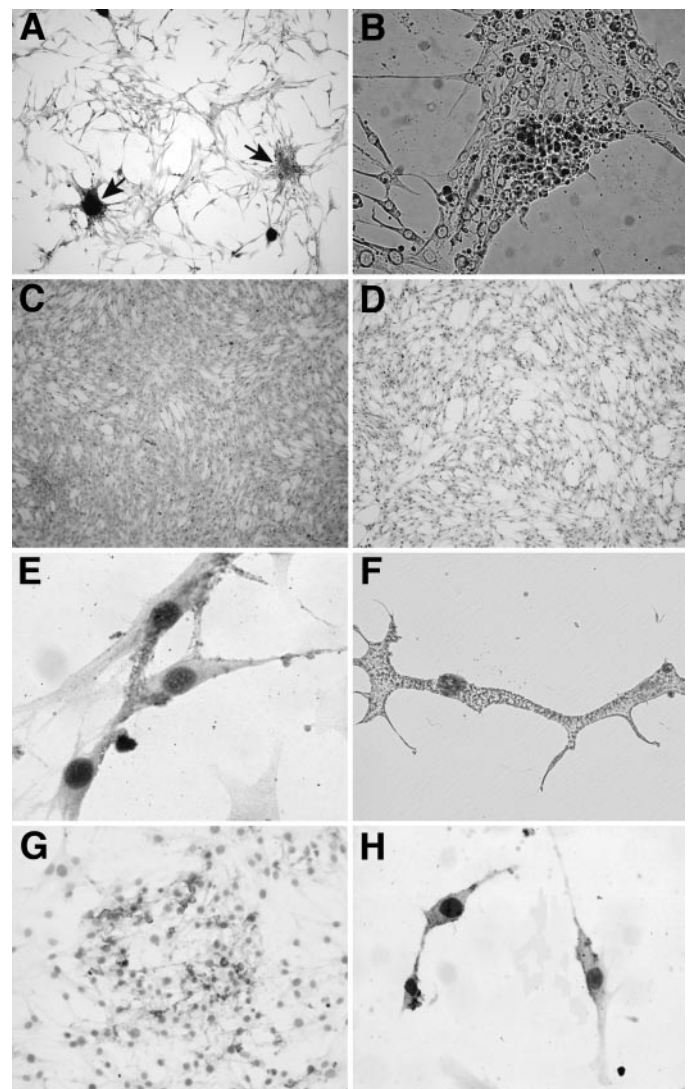
teocytes, adipocytes, and cells of neuronal lineage (Figure 8). When cloned cells were cultured with MDI-I mixture for 21 d, most of the cells (95% per plate) showed cytoplasmic accumulation of oil droplets stained with Oil-Red O, indicating that Sca-1$^+$ cells differentiated into adipocytes (Figure 8, B and B1). When treated with osteogenic inducers, 21 d after induction, a large population of cells (95% per plate) showed the presence of alkaline phosphatase, one of the early markers of osteogenesis, and stained positive with calcium-binding alizarin red, both indicating osteogenic differentiation (Figure 8, D and F). After induction, neuronal lineage differentiation of renal Sca-1$^+$Lin$^-$ cells was confirmed by staining with nestin and β-tubulin III. Although neuronal-like projections were visible in cultures,
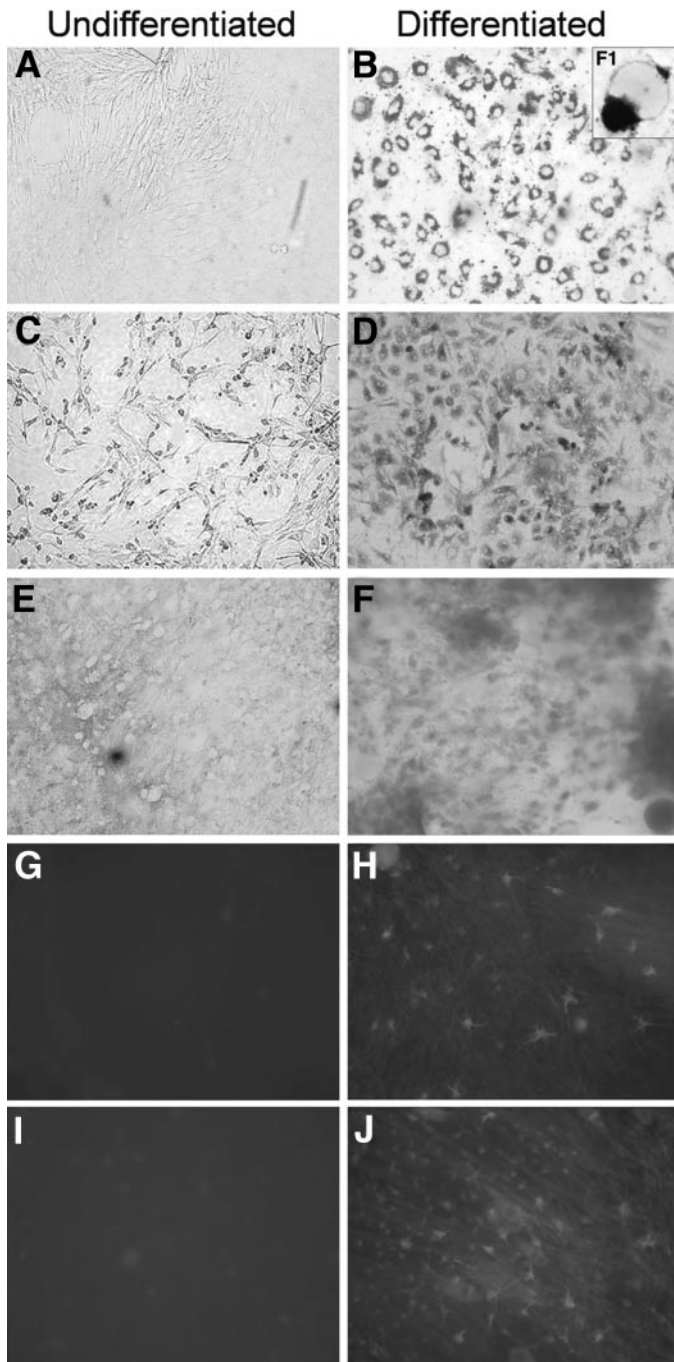
Figure 8. Clonal derivation of adipogenic, osteogenic, and neuronal lineages. Highly efficient differentiation of cloned renal Sca-1$^+$Lin$^-$ cells (90 to 95% of plated cells) into adipogenic (B and inset B1), osteogenic (D and F), and neuronal lineages (H and J) is demonstrated. Cell differentiation in these cultures of cloned cells was observed after staining with oil red O (A and B, red-orange), nitro blue tetrazolium (C and D, blue), and alizarin red (E and F, red) and by immunostaining with an antibody specific for nestin (G and H, red) and for β-tubulin III (I and J, red). Magnification, ×10.

>90% of the cells stained positively for both nestin (Figure 8H) and β-tubulin III (Figure 8J), confirming the neuronal identity of these cells. In all instances, control medium failed to induce

adipogenic, osteogenic, and neuronal differentiation (Figure 8, A, C, E, G, and I, respectively). Under these same conditions, BM-derived MSC differentiated into the mesodermal cell types at comparable frequencies (data not shown), whereas control 3T3 mature fibroblasts could be differentiated into adipocytes but not to any other cell type. Thus, the renal Sca-1$^+$Lin$^-$ cells are multipotent and demonstrate remarkable plasticity.

Microarray Analysis of Renal Sca-1$^+$Lin$^-$ Cells

After identification of a distinct progenitor cell phenotype in the adult kidney, we investigated the molecular phenotype of these cells, which might clarify better their biologic properties. MOE430 A 2.0 Affymetrix microarrays that contained 22,690 probe sets were used to identify genes that were enriched in interstitial Sca-1$^+$ cells *via* MACS, in comparison with the more differentiated cells of the Sca-1$^-$ fraction (each obtained from three independent experiments). A total of 10,212 "valid genes," characterized by probe sets showing "present" calls and intensity signals above 20 in either three Sca-1$^+$ or Sca-1$^-$ replicates, were filtered further to discriminate differentially expressed genes. This set of data is available at http://eng.she-ba.co.il/genomics. A total of 1193 probe sets discriminated between the Sca-1$^+$ and Sca-1$^-$ samples ($P < 0.05$), representing 1053 genes, 336 of which were upregulated in the Sca-1$^+$ samples, whereas 717 genes were downregulated. This set of data is available as supplementary material.

Microarray profiling (Table 2) was concordant with the FACS analysis of cell surface markers, specifically showing genes encoding for lymphocyte antigen 6 complex, locus A (Sca-1), and integrin-β1 (CD29) to be significantly upregulated in the Sca-1$^+$ fraction, and adding the tetraspanin (CD151) and transferrin receptor (CD71) as surface markers that are present. Sca-1$^+$ cells were enriched for multiple transcriptional repressors and cellular quiescence genes (Hipk2, Max1, Nf2, Ndr2, Sav1, quiescin Q6, and klotho [33–39]) as well as genes that participate in resistance to stress, with upregulated detoxifier systems and antioxidative genes (Table 2). These along with TGF-β, Yes (Yamaguchi sarcoma), and gp130 (IL6st) signaling and the interaction with the extracellular matrix *via* integrin-β1 and Adam9 (all upregulated in the Sca-1$^+$ cells) are essential attributes of the recently described core stem cell properties (or "stemness") (40). It is interesting that renal Sca-1$^+$ cells overexpress developmental pathways that are associated with mesoderm lineage formation. These include members of the TGF-β/bone morphogenic protein (BMP) family, which prompt efficient myogenesis and osteogenesis (41); furin, a TGF-β1 activator; TGF-β receptor II; and Sitpec/Ecsit, which associates with Smad1 and Smad4 and is required for BMP signaling and mesoderm formation during mouse embryogenesis (42,43). Accordingly, a variety of muscle and bone genes that are implicated in these tissues' formation are upregulated in renal Sca-1$^+$ cells: Myocyte enhancer factor 2A and YY1-associated factor 2 (YAF2) (myocardiogenic transcription factors that have been shown to be critically involved in the development and phenotype regulation of skeletal and cardiac muscle [44–46]); Filamin-β (filamentous actin cross-linking protein, which accelerates differentiation into myotubes [47]); calumenin and frac-

Table 2. Genes induced in renal Sca-1$^+$Lin$^-$ cells and placed into functional categories[a]

Development and differentiation: Sitpec, Tgfbr2, Fgfr1, Lrp6, Anpep, Flnb, Pafah1b1, Spnr, Ndr2, Kl, Asah2, Ndfip1, Rtn3
Regulation of transcription and cell cycle: Mef2a, Yaf2, Hipk2, Mxi1, Nr1 h2, Rab2, Phf10, v-yes, Nf2, Mad2l2, Nras, Rad21, Sav1, Sycp3, Cnnm2
Adhesion and extracellular matrix: Itgb1, Cd47, Cd151, Scarb2, Adam9, Sdf4, Col4a4, Ext2
Cytoskeleton organization and motility: Myo1c, Arpc5, Arpc3, Tuba6, Rsn, Pafah1b1, Strbp, Lasp1, Ank3, Ocln, Dock8
Signal transduction: Cell surface receptor linked: Il6st, M6pr, Insig2, Gpsm2, Sitpec, Tgfbr2, Lrp6, Itgb1, Fgfr1; other, Yes, Rab6, Rab2, Rheb, Sara2, Nras, Pkig, Itpk1
Cell death: Pdcd6, Bcap31, Tegt, Faf1, Tde1, Sh3glb1, Scotin, Ddx52
Metabolism: Cct7, Mrpl20, Mrpl17, Mrpl44, Ddost, Prss11, Man1a, Furin, B3gnt1, Galnt2, Psma7, Dnajc3, P4 hb, Itm1, Gpd2, Cdipt, Ptdss1, Ptdss2
Transport: Fxc1, Calu Lamp1, Laptm4a, Laptm4b, Fkbp1a, Scamp2, Bet1, Tmem9, Arf4, Arf3, Lman1, Mcfd2, Ywhaz, Trfr
Ion transport: Atp1b1, Atp6v0e, Slc22a1l, Slc22al2, Slc10a3, Slc41a1, Car4
Cell stress and defense: Serpinh1, Ndufb9, Ndufb4, Ndufa1, Ndufab1, Cox8a, Cox7c, Cox7a2, Enpep, Ifi30, Cklfsf6, Cyb561
Unknown: Mkrn2, Tex2, Tes3, Ttc13, Srd5a2l

[a]A total of 336 transcripts were significantly upregulated ($P < 0.05$) in renal Sca-1$^+$ cells compared with Sca-1$^-$ cells; relevant transcripts with a 1.5-fold or greater change in average signal intensity are shown.

tured callus expressed, which are elevated in the early stages of a healing fracture and during differentiation along the osteoblast lineage; and exotoses (multiple)2, implicated in heparan sulfate proteoglycans synthesis and bone overgrowth (48–50). In addition, 6MPR/IGFIIR, insulin-induced gene 2, and Prss11 (IGF-binding protein protease), which promote adipogenic differentiation, are overexpressed in renal Sca-1$^+$ cells (51,52). Other developmental signaling pathways might be active in renal Sca-1$^+$ cells on the basis of the expression of specific genes, such as LRP6, a critical mediator of Wnt signaling in mice (53), and FGFR1 (54). Finally, overexpression of a variety of genes that are involved in cell adhesion, motility, and cytoskeleton assembly (*e.g.*, Lasp1, Arpc3, Arpc5, nonmuscle Myosin IC) suggests a phenotype of migrating cells, a feature that is required if renal Sca-1$^+$ cells were to participate in tissue repair.

Renal Sca-1$^+$Lin$^-$ Cells Exhibit a Potent Immune Regulatory Effect

MSC have been shown to have an immune-privileged behavior (55). We therefore assessed possible an immunomodulatory

role of renal Sca-1$^+$Lin$^-$ cells. Splenocytes from 2c transgenic mice (H-2^b), bearing transgene TCR specific against H-2^d, were stimulated in one-way mixed lymphocyte reaction (MLR) against DBA/2 splenocytes (H-2^d). Expression of 1B2$^+$ CD8 T cells was analyzed by FACS. Inhibition of expansion of 1B2$^+$ CD8 T cells after addition to the MLR culture of newly isolated or 30-d cultured renal Sca-1$^+$Lin$^-$ cells from DBA/2 (H-2^d) and SJL mice (H-2^s) was determined at 48 h after initiation of the MLR and compared with that observed when adding fresh BM and MSC (30 d in culture; Figure 9). As shown, whereas freshly isolated cells demonstrated a reduction in 1B2$^+$ CD8 T cells only in the higher concentration (1:10), addition of cultured renal Sca-1$^+$ cells led to a markedly reduced number of activated alloreactive CD8 T cells. This effect is comparable to that observed for MSC. In all instances, this inhibition of cell expansion in MLR of CD8 T cells was nonspecific (not *via* H-2 recognition), because cells that originated from DBA/2 and SJL mice showed similar effects. These results illustrating the potent immune regulatory effect of cultured renal Sca-1$^+$ cells are consistent with the recently described general immunosuppressive effects of MSC (55). The finding that the immunomodulatory effects of MSC are regulated by prostaglandin E2, which is constitutively produced and secreted by MSC in culture (55), might explain our observations in cultured *versus* fresh renal Sca-1$^+$ cells.

Renal Sca-1$^+$ Cells Adopt a Tubular Phenotype after I/R Injury

In proof-of-concept studies to explore the feasibility of renal Sca-1$^+$ cells to contribute to the repair of the kidney after I/R injury, we isolated an enriched nontubular renal Sca-1$^+$Lin$^-$ cell fraction from Rosa26 mice, which carry the bacterial *lacZ* gene (LacZ$^+$Sca-1$^+$ cells), making it possible to identify transplanted donor cells in the recipient mice by staining for β-galactosidase activity (X-gal staining) or immunostaining for the β-gal epitope. Taking into account that X-gal stains tubular cells in kidneys of wild-type mice, reflecting endogenous β-gal activity, we chose to perform immunostaining of paraffin sections using anti–β-gal antibodies, which can distinguish bacterial from endogenous β-gal (56). Figure 10, A and B, demonstrates immunostaining of a ROSA26 kidney. Cells were filtered before their use and injected through the renal pelvis into the renal parenchyma (2.0 × 10^6 cells per mouse; $n = 6$) immediately after the ischemic period. We evaluated for the presence of β-gal$^+$ donor cells in host kidneys 1 mo after injection so as to eliminate transient engraftment of cells. Sections of kidneys from mice that had undergone ischemic injury and were treated with freshly isolated renal Sca-1$^+$ cells revealed positive β-gal immunostaining within the regenerating renal tubules. The majority of these tubules were confined to the region of cell injection in the deep layers of the medulla (Figure 10C). It is interesting that we found that individual epithelial cells within the tubules expressed β-gal rather than whole tubules (Figure 10, D and E). Although this phenomenon could be the result of renal progenitor cell differentiation and individual cell engraftment and replacement, it also may arise from fusion to host cells (15,16) and therefore should be interpreted cautiously. In
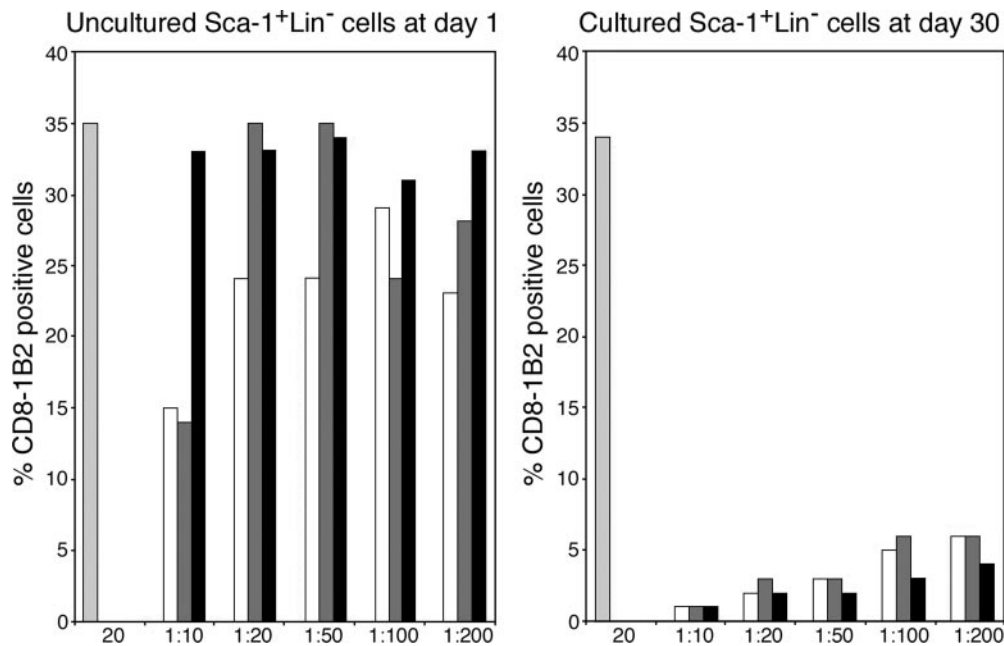
Figure 9. Immune regulatory effects of renal Sca-1+Lin− cells. The inhibitory effect of renal Sca-1+Lin− cells was studied by one-way MLR in the 2C transgenic animal model. Splenocytes from 2C transgenic mice (H-2b) bearing transgene T cell receptor (TCR) specific against H-2d (1B2+) were stimulated in MLR against DBA/2 splenocytes (H-2d). FACS analysis shows the frequency of 1B2+ CD8 T cells in the absence (2C control, no inhibition; ▨) or the presence of newly isolated (left) and 30-d cultured (right) renal Sca-1+Lin− cells of DBA/2 origin (□) or SJL origin (dark gray bars). The effects of whole bone marrow (BM) cells (left) and mesenchymal stem cells (right) of DBA/2 origin (■) were analyzed for comparison. Data are shown 3 d after initiation of the mixed lymphocyte reaction.

addition, we found few β-gal+ cells engrafted in the interstitial space (Figure 10F). In control sections of kidneys that were subjected to ischemic injury and vehicle injection (Sca-1− cells), as well as intact kidneys, we failed to detect β-gal–expressing cells in corresponding regions (Figure 10, E and F). Therefore, Sca-1+Lin−CD45− cells of the adult kidney are capable of populating the renal tubule after ischemic injury.

Discussion

Although the mammalian kidney has an intrinsic regenerative potential and it is not a terminally differentiated organ, tissue-resident adult renal stem cell populations remain enigmatic (57). The classic approach to isolation of stem cells from BM has been based on the use of surface markers and their respective antibodies. The lack of known cell surface markers for renal progenitor cells has limited the use of such an approach with the kidney. We therefore used sorting for Sca-1, which has been shown to characterize adult BM and tissue stem cells (20–25,57).

Our results using FACS to analyze renal cell suspension from adult mice showed a highly reproducible population termed "lymphogate" on the basis of size and granularity. When a sample of spleen was subjected to the same staining and run through the cell sorter immediately before a kidney sample, the renal lymphogate was found to be in the same gated region as the spleen lymphogate. In contrast with the spleen cells, further FACS analysis of the kidney lymphogate separated these cells into hematopoietic and nonhematopoietic fractions on the basis

of the presence or absence, respectively, of the pan-leukocyte cell surface marker CD45. The CD45− fraction was shown to express Sca-1 and was hypothesized to include the renal stem cells. This cell fraction is greatly enriched by Sca-1 magnetic cell sorting. Because Sca-1 has been reported to present in renal epithelial tubular cells, it was important to assess by additional FACS sorting whether the gated fraction included epithelial cells. The mesenchymal nature of the gated CD45−Sca-1+ cell fraction was confirmed after sorting and phenotypical characterization that showed these cells to be positive for vimentin and negative for cytokeratin. Furthermore, morphologic examination showed that this cell fraction is not homogenous, containing at least two subpopulations that could be sorted further on the basis of Sca-1 expression into Sca-1dim and less frequent Sca-1bright cells. The latter were shown to be a population of highly adherent small round cells, which transform into fibroblast-like cells in culture. A similar cell phenotype also can be obtained after culture of the enriched nontubular Sca-1 population that was obtained by magnetic sorting and elimination of the nonadherent fraction. Therefore, it seems that additional FACS sorting of the kidney preparations according to size and granularity yields a fraction that includes both the putative stem cells and significant numbers of non–stem cells, and sorting for Sca-1bright cells within the lymphogate will be advantageous. Clearly, the ability to isolate these cells constitutes a critical step in being able to observe, characterize, and understand them in future studies.

Whereas significantly expressing CD29 (β1-integrin), the
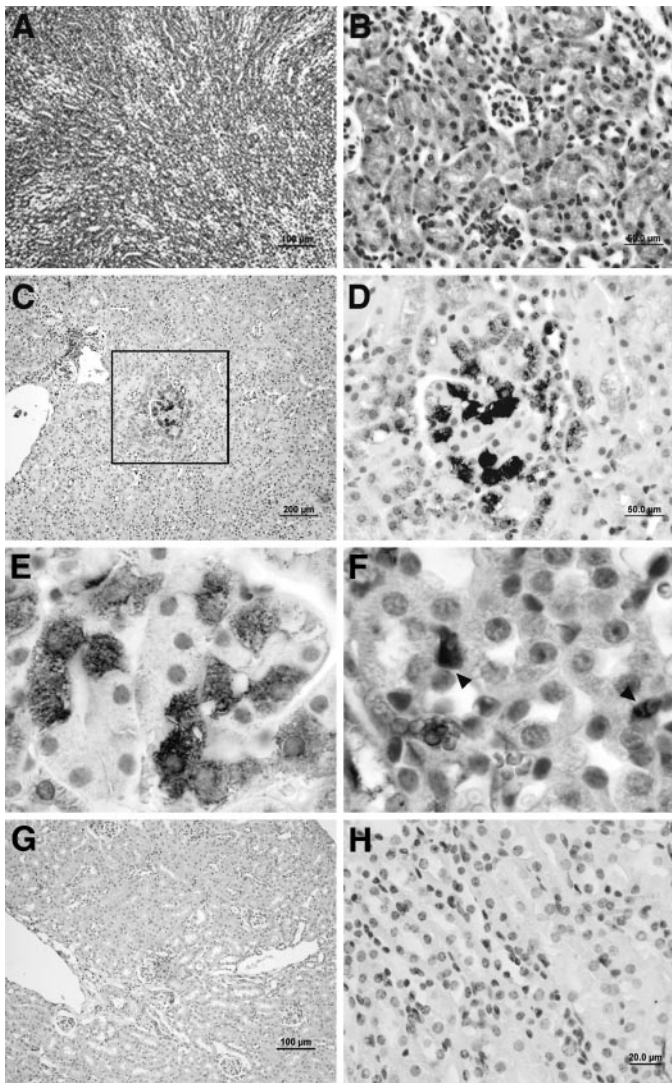
Figure 10. Contribution of renal Sca-1$^+$Lin$^-$ progenitor cells to kidney repair. Cells were obtained from ROSA26 transgenic mice and injected directly into kidneys of C57BL/6 wild-type mice. (A and B) Immunostaining for LacZ was performed in control ROSA26 transgenic kidneys cells; note uniform positive staining. (C through F) Sections of kidney from C57BL/6 wild-type mouse 4 wk after ischemia/reperfusion (I/R) injury and transplantation of renal Sca-1$^+$Lin$^-$ cells shown in low magnification (C and D) and high magnification (E and F); note positive staining in individual tubular cells (E) and interstitial cells (F, arrowheads). (G and H) Control C57BL/6 kidney subjected to I/R injury and injection of renal Sca-1$^-$ cells; note lack of staining of LacZ in corresponding deep regions. Magnifications: ×10 in A, C, and G; ×40 in B, D, and H; ×100 in E and F.

nontubular Sca-1$^+$ cells showed little to no expression of several markers that are known to be present on other stem cells. For example, CD44, CD90, CD34, and c-kit, which are known to be enriched in BM mesenchymal and hematopoietic progenitor cells, were not expressed in the gated renal Sca-1$^+$ cells (2,25). Therefore, we conclude that these CD45$^-$Lin$^-$Sca-1$^+$ cells are

different phenotypically from stem cells of BM but similar to those observed in other tissues, in particular, multipotential myogenic and cardiogenic progenitor cells in the interstitium of skeletal muscle and myocardium that are Sca-1$^+$ but CD45$^-$, CD34$^-$, and c-Kit$^-$ (20,21,58). We have identified Sca-1$^+$ cells in the kidney interstitium in close proximity to tubules, most notably in the renal papilla. During preparation of this article, putative adult kidney stem cells were isolated with the aid of side population FACS sorting (59). It is interesting that the kidney side population cells, which were shown to promote kidney regeneration, reside in the interstitial space and are Sca-1$^+$ (>70% on average) but CD45$^-$. In addition, populations of renal papillary cells were suggested as stem cells on the basis of the their ability to retain bromodeoxyuridine (label-retaining or low-cycling cells) (60). These cells, which were shown to be located mostly in the interstitium of the renal papilla, were phenotypically negative for CD45, CD34, CD44, or c-Kit (Sca-1 was not evaluated). Therefore, shared phenotypic features suggest that the nontubular Sca-1$^+$Lin$^-$ cells may resemble not only resident cardiac and skeletal stem cells but also several proposed renal progenitor populations.

Recently, Verfaillie and co-workers (61), who previously identified multipotent adult progenitor cells that co-purify with MSC in postnatal BM, extended their findings into solid organs. Accordingly, cells that were cultured from muscle and brain (negative for CD44, CD45, major MHC classes I and II, and c-kit) differentiated to mesodermal, neuronal, and endodermal cell types (62). These cells, which originally were derived from BM, might circulate and home to stem cell niches. In fact, Dreyfus *et al.* (63) recently showed that multipotent CD45$^-$Sca-1–expressing cells that are located in muscle connective tissue can derive from BM in adulthood, constituting a reservoir of interstitial stem cells. It is interesting that many known genes that are overexpressed in the renal Sca-1$^+$ microarrays belong to response pathways to developmental signaling molecules, such as Wnt, TGF-β/BMP, and FGF. These pathways, critical for self-renewal of stem cells (64), have been shown to be overexpressed in mesoderm progenitor cells of fetal origin, termed mesoangioblasts, in which they activate differentiation programs. Future studies using the formation of BM chimeras and lineage-tracking analysis can establish lineage relationships of the nontubular renal Sca-1$^+$ progenitors and determine whether they are intrinsic to the organ (*i.e.*, reside and self-renew in the kidney from early embryonic stages) or rather migrate at other developmental stages.

Recent studies have suggested that a significant part of the replenishment of the tubular epithelium after ischemia derives from intrinsic tubular cell proliferation rather than BM-derived cells (56,65). Indeed, transplantation of human HSC in ischemic kidneys suggests a role in vasculogenesis but not tubulogenesis (66). Because large numbers of proliferating cells are observed early after ischemic injury at diverse sites in the regenerating tubules, Duffield *et al.* (56) challenged the presence of endogenous kidney stem cells by arguing that a large population of such cells would have to be adjacent to tubules to give to their rise. Indeed, after ischemic injury and intrarenal injection of an enriched fraction of nontubular Sca-1$^+$ cells, we observed lo-

calized rather than diffuse engraftment in tubular cells; therefore, contribution to tubular repair probably is minor compared with intrinsic tubular cell proliferation. Isolation, expansion, and delivery of the Sca-1^{high} cells into injured kidneys might provide improved results. In any case, the beneficial effects of nontubular Sca-1$^+$Lin$^-$ cells might be mediated by their ability to supply large amounts of angiogenic, antiapoptotic, and mitogenic factors in kidney disease (67). Furthermore, the multipotency of the cells and their immune regulatory potential call for their evaluation in both autologous and allogeneic models of injury that do not afflict the kidneys (*e.g.*, heart infarct, neurodegenerative disease).

Acknowledgments

References

1. Fodor WL: Tissue engineering and cell based therapies, from the bench to the clinic: The potential to replace, repair and regenerate. *Reprod Biol Endocrinol* 1: 102, 2003
2. Kondo M, Wagers AJ, Manz MG, Prohaska SS, Scherer DC, Beilhack GF, Shizuru JA, Weissman IL: Biology of hematopoietic stem cells and progenitors: Implications for clinical application. *Annu Rev Immunol* 21: 759–806, 2003
3. Fibbe W: Mesenchymal stem cells. A potential source for skeletal repair. *Ann Rheum Dis* 61[Suppl 2]: ii29–ii31, 2002
4. Lagasse E, Connors H, Al-Dhalimy M, Reitsma M, Dohse M, Osborne L, Wang X, Finegold M, Weissman IL, Grompe M: Purified hematopoietic stem cells can differentiate into hepatocytes in vivo. *Nat Med* 6: 1229–1234, 2000
5. Mezey E, Chandross KJ, Harta G, Maki RA, McKercher SR: Turning blood into brain: Cells bearing neuronal antigens generated in vivo from bone marrow. *Science* 290: 1779–1782, 2000
6. Ianus A, Holz GG, Theise ND, Hussain MA: In vivo derivation of glucose-competent pancreatic endocrine cells from bone marrow without evidence of cell fusion. *J Clin Invest* 111: 843–850, 2003
7. Badiavas EV, Abedi M, Butmarc J, Falanga V, Quesenberry P: Participation of bone marrow derived cells in cutaneous wound healing. *J Cell Physiol* 196: 245–250, 2003
8. Okamoto R, Yajima T, Yamazaki M, Kanai T, Mukai M, Okamoto S, Ikeda Y, Hibi T, Inazawa J, Watanabe M: Damaged epithelia regenerated by bone marrow-derived cells in the human gastrointestinal tract. *Nat Med* 8: 1011–1017, 2002
9. Poulsom R, Forbes SJ, Hodivala-Dilke K, Ryan E, Wyles S, Navaratnarasah S, Jeffery R, Hunt T, Alison M, Cook T, Pusey C, Wright NA: Bone marrow contributes to renal parenchymal turnover and regeneration. *J Pathol* 195: 229–235, 2001
10. Kale S, Karihaloo A, Clark PR, Kashgarian M, Krause DS, Cantley LG: Bone marrow stem cells contribute to repair of

11. Lin F, Cordes K, Li L, Hood L, Couser WG, Shankland SJ, Igarashi P: Hematopoietic stem cells contribute to the regeneration of renal tubules after renal ischemia-reperfusion injury in mice. *J Am Soc Nephrol* 14: 1188–1199, 2003
12. Wagers AJ, Sherwood RI, Christensen JL, Weissman IL: Little evidence for developmental plasticity of adult hematopoietic stem cells. *Science* 297: 2256–2259, 2002
13. Choi JB, Uchino H, Azuma K, Iwashita N, Tanaka Y, Mochizuki H, Migita M, Shimada T, Kawamori R, Watada H: Little evidence of transdifferentiation of bone marrow-derived cells into pancreatic beta cells. *Diabetologia* 46: 1366–1374, 2003
14. Terada N, Hamazaki T, Oka M, Hoki M, Mastalerz DM, Nakano Y, Meyer EM, Morel L, Petersen BE, Scott EW: Bone marrow cells adopt the phenotype of other cells by spontaneous cell fusion. *Nature* 416: 542–545, 2002
15. Wang X, Willenbring H, Akkari Y, Torimaru Y, Foster M, Al-Dhalimy M, Lagasse E, Finegold M, Olson S, Grompe M: Cell fusion is the principal source of bone-marrow-derived hepatocytes. *Nature* 422: 897–901, 2003
16. Alvarez-Dolado M, Pardal R, Garcia-Verdugo JM, Fike JR, Lee HO, Pfeffer K, Lois C, Morrison SJ, Alvarez-Buylla A: Fusion of bone-marrow-derived cells with Purkinje neurons, cardiomyocytes and hepatocytes. *Nature* 425: 968–973, 2003
17. Rookmaaker MB, Smits AM, Tolboom H, Van 't Wout K, Martens AC, Goldschmeding R, Joles JA, Van Zonneveld AJ, Grone HJ, Rabelink TJ, Verhaar MC: Bone-marrow-derived cells contribute to glomerular endothelial repair in experimental glomerulonephritis. *Am J Pathol* 163: 553–562, 2003
18. Ito T, Suzuki A, Imai E, Okabe M, Hori M: Bone marrow is a reservoir of repopulating mesangial cells during glomerular remodeling. *J Am Soc Nephrol* 12: 2625–2635, 2001
19. Cornacchia F, Fornoni A, Plati AR, Thomas A, Wang Y, Inverardi L, Striker LJ, Striker GE: Glomerulosclerosis is transmitted by bone marrow-derived mesangial cell progenitors. *J Clin Invest* 108: 1649–1656, 2001
20. Oh H, Bradfute SB, Gallardo TD, Nakamura T, Gaussin V, Mishina Y, Pocius J, Michael LH, Behringer RR, Garry DJ, Entman ML, Schneider MD: Cardiac progenitor cells from adult myocardium: Homing, differentiation, and fusion after infarction. *Proc Natl Acad Sci U S A* 100: 12313–12318, 2003
21. Asakura A, Seale P, Girgis-Gabardo A, Rudnicki MA: Myogenic specification of side population cells in skeletal muscle. *J Cell Biol* 159: 123–134, 2002
22. Tamaki T, Akatsuka A, Ando K, Nakamura Y, Matsuzawa H, Hotta T, Roy RR, Edgerton VR: Identification of myogenic-endothelial progenitor cells in the interstitial s of skeletal muscle. *J Cell Biol* 157: 571–577, 2002
23. Welm BE, Tepera SB, Venezia T, Graubert TA, Rosen JM, Goodell MA: Sca-1(pos) cells in the mouse mammary gland represent an enriched progenitor cell population. *Dev Biol* 245: 42–56, 2002
24. Howell JC, Yoder MC, Srour EF: Hematopoietic potential of murine skeletal muscle-derived CD45(−)Sca-1(+)c-kit(−) cells. *Exp Hematol* 30: 915–924, 2002
25. Anjos-Afonso F, Siapati EK, Bonnet D: In vivo contribution of murine mesenchymal stem cells into multiple cell-types

the ischemically injured renal tubule. *J Clin Invest* 112: 42–49, 2003

under minimal damage conditions. *J Cell Sci* 117: 5655–5664, 2004

26. Epting CL, Lopez JE, Shen X, Liu L, Bristow J, Bernstein HS: Stem cell antigen-1 is necessary for cell-cycle withdrawal and myoblast differentiation in C2C12 cells. *J Cell Sci* 117: 6185–6195, 2004

27. van de Rijn M, Heimfeld S, Spangrude GJ, Weissman IL: Mouse hematopoietic stem-cell antigen Sca-1 is a member of the Ly-6 antigen family. *Proc Natl Acad Sci U S A* 86: 4634–4638, 1989

28. Kotton DN, Summer RS, Sun X, Ma BY, Fine A: Stem cell antigen-1 expression in the pulmonary vascular endothelium. *Am J Physiol Lung Cell Mol Physiol* 284: L990–L996, 2003

29. Dekel B, Burakova T, Arditti FD, Reich-Zeliger S, Milstein O, Aviel-Ronen S, Rechavi G, Friedman N, Kaminski N, Passwell JH, Reisner Y: Human and porcine early kidney precursors as a new source for transplantation. *Nat Med* 9: 53–60, 2003

30. Oliver JA, Barasch J, Yang J, Herzlinger D, Al-Awqati Q: Metanephric mesenchyme contains embryonic renal stem cells. *Am J Physiol Renal Physiol* 283: F799–F809, 2002

31. Almeida-Porada G, El Shabrawy D, Porada C, Zanjani ED: Differentiative potential of human metanephric mesenchymal cells. *Exp Hematol* 30: 1454–1462, 2002

32. Dekel B, Hochman E, Sanchez MJ, Maharshak N, Amariglio N, Green AR, Izraeli S: Kidney, blood and endothelium: Developmental expression of stem cell leukemia during nephrogenesis. *Kidney Int* 65: 1162–1169, 2004

33. Takahashi Y, Kuro-O M, Ishikawa F: Aging mechanisms. *Proc Natl Acad Sci U S A* 97: 12407–12408, 2000

34. Coppock D, Kopman C, Gudas J, Cina-Poppe DA: Regulation of the quiescence-induced genes: Quiescin Q6, decorin, and ribosomal protein S29. *Biochem Biophys Res Commun* 269: 604–610, 2000

35. Tapon N, Harvey KF, Bell DW, Wahrer DC, Schiripo TA, Haber DA, Hariharan IK: Salvador promotes both cell cycle exit and apoptosis in *Drosophila* and is mutated in human cancer cell lines. *Cell* 110: 467–478, 2002

36. Satterwhite DJ, White RL, Aakre ME, Moses HL: TGF-beta1 regulates the expression of multiple max-interacting transcription factors in Balb/MK cells: Implications for understanding the mechanism of action of TGF-beta1. *Pediatr Res* 50: 67–75, 2001

37. Pierantoni GM, Bulfone A, Pentimalli F, Fedele M, Iuliano R, Santoro M, Chiariotti L, Ballabio A, Fusco A: The homeodomain-interacting protein kinase 2 gene is expressed late in embryogenesis and preferentially in retina, muscle, and neural tissues. *Biochem Biophys Res Commun* 290: 942–947, 2002

38. Lohez OD, Reynaud C, Borel F, Andreassen PR, Margolis RL: Arrest of mammalian fibroblasts in G1 in response to actin inhibition is dependent on retinoblastoma pocket proteins but not on p53. *J Cell Biol* 161: 67–77, 2003

39. Deng Y, Yao L, Chau L, Ng SS, Peng Y, Liu X, Au WS, Wang J, Li F, Ji S, Han H, Nie X, Li Q, Kung HF, Leung SY, Lin MC: N-Myc downstream-regulated gene 2 (NDRG2) inhibits glioblastoma cell proliferation. *Int J Cancer* 106: 342–347, 2003

40. Ramalho-Santos M, Yoon S, Matsuzaki Y, Mulligan RC, Melton DA: "Stemness": Transcriptional profiling of embryonic and adult stem cells. *Science* 298: 597–600, 2002

41. Tagliafico E, Brunelli S, Bergamaschi A, De Angelis L, Scardigli R, Galli D, Battini R, Bianco P, Ferrari S, Cossu G, Ferrari S: TGFbeta/BMP activate the smooth muscle/bone differentiation programs in mesoangioblasts. *J Cell Sci* 117: 4377–4388, 2004

42. Dubois CM, Blanchette F, Laprise MH, Leduc R, Grondin F, Seidah NG: Evidence that furin is an authentic transforming growth factor-beta1-converting enzyme. *Am J Pathol* 158: 305–316, 2001

43. Xiao C, Shim JH, Kluppel M, Zhang SS, Dong C, Flavell RA, Fu XY, Wrana JL, Hogan BL, Ghosh S: Ecsit is required for Bmp signaling and mesoderm formation during mouse embryogenesis. *Genes Dev* 17: 2933–2949, 2003

44. Lemonnier M, Buckingham ME: Characterization of a cardiac specific enhancer which directs alpha-cardiac actin gene transcription in the mouse adult heart. *J Biol Chem* 279: 55651–55658, 2004

45. Rauch C, Loughna PT: Static stretch promotes in a calcineurin and p38 dependent manner MEF2A nuclear translocation and expression of neonatal myosin heavy chain in C2C12 myocytes *Am J Physiol Cell Physiol* 288: C593–C605, 2005

46. Kalenik JL, Chen D, Bradley ME, Chen SJ, Lee TC: Yeast two-hybrid cloning of a novel zinc finger protein that interacts with the multifunctional transcription factor YY1. *Nucleic Acids Res* 25: 843–849, 1997

47. van der Flier A, Kuikman I, Kramer D, Geerts D, Kreft M, Takafuta T, Shapiro SS, Sonnenberg A: Different splice variants of filamin-B affect myogenesis, subcellular distribution, and determine binding to integrin beta subunits. *J Cell Biol* 156: 361–376, 2002

48. Nakazawa T, Nakajima A, Seki N, Okawa A, Kato M, Moriya H, Amizuka N, Einhorn TA, Yamazaki M: Gene expression of periostin in the early stage of fracture healing detected by cDNA microarray analysis. *J Orthop Res* 22: 520–525, 2004

49. Hadjiargyrou M, Halsey MF, Ahrens W, Rightmire EP, McLeod KJ, Rubin CT: Cloning of a novel cDNA expressed during the early stages of fracture healing. *Biochem Biophys Res Commun* 249: 879–884, 1998

50. Bornemann DJ, Duncan JE, Staatz W, Selleck S, Warrior R: Abrogation of heparan sulfate synthesis in *Drosophila* disrupts the Wingless, Hedgehog and Decapentaplegic signaling pathways. *Development* 131: 1927–1938, 2004

51. Lee S, Lee DK, Choi E, Lee JW: Identification of a functional vitamin D response element in the murine Insig-2 promoter and its potential role in the differentiation of 3T3–L1 preadipocytes. *Mol Endocrinol* 19: 399–408, 2005

52. Hou J, Clemmons DR, Smeekens S: Expression and characterization of a serine protease that preferentially cleaves insulin-like growth factor binding protein-5. *J Cell Biochem* 94: 470–484, 2005

53. Pinson KI, Brennan J, Monkley S, Avery BJ, Skarnes WC: An LDL-receptor-related protein mediates Wnt signalling in mice. *Nature* 407: 535–538, 2000

54. Stachowiak EK, Fang X, Myers J, Dunham S, Stachowiak MK: cAMP-induced differentiation of human neuronal progenitor cells is mediated by nuclear fibroblast growth factor receptor-1 (FGFR1). *J Neurochem* 84: 1296–1312, 2003

55. Aggarwal S, Pittenger MF: Human mesenchymal stem cells modulate allogeneic immune cell responses. *Blood* 105: 1815–1822, 2005

56. Duffield JS, Park KM, Hsiao LL, Kelley VR, Scadden DT, Ichimura T, Bonventre JV: Restoration of tubular epithelial cells during repair of the postischemic kidney occurs independently of bone marrow-derived stem cells. *J Clin Invest* 115: 1743–1755, 2005

57. Wagers AJ, Weissman IL: Plasticity of adult stem cells. *Cell* 116: 639–648, 2004

58. Seale P, Asakura A, Rudnicki MA: The potential of muscle stem cells. *Dev Cell* 1: 333–342, 2001

59. Hishikawa K, Marumo T, Miura S, Nakanishi A, Matsuzaki Y, Shibata K, Ichiyanagi T, Kohike H, Komori T, Takahashi I, Takase O, Imai N, Yoshikawa M, Inowa T, Hayashi M, Nakaki T, Nakauchi H, Okano H, Fujita T: Musculin/MyoR is expressed in kidney side population cells and can regulate their function. *J Cell Biol* 169: 921–928, 2005

60. Oliver JA, Maarouf O, Cheema FH, Martens TP, Al-Awqati Q: The renal papilla is a niche for adult kidney stem cells. *J Clin Invest* 114: 795–804, 2004

61. Jiang Y, Jahagirdar BN, Reinhardt RL, Schwartz RE, Keene CD, Ortiz-Gonzalez XR, Reyes M, Lenvik T, Lund T, Blackstad M, Du J, Aldrich S, Lisberg A, Low WC, Largaespada DA, Verfaillie CM: Pluripotency of mesenchymal stem cells derived from adult marrow. *Nature* 418: 41–49, 2002

62. Jiang Y, Vaessen B, Lenvik T, Blackstad M, Reyes M, Verfaillie CM: Multipotent progenitor cells can be isolated from postnatal murine bone marrow, muscle, and brain. *Exp Hematol* 30: 896–904, 2002

63. Dreyfus PA, Chretien F, Chazaud B, Kirova Y, Caramelle P, Garcia L, Butler-Browne G, Gherardi RK: Adult bone marrow-derived stem cells in muscle connective tissue and satellite cell niches. *Am J Pathol* 164: 773–779, 2004

64. Varga AC, Wrana JL: The disparate role of BMP in stem cell biology. *Oncogene* 24: 5713–5721, 2005

65. Lin F, Moran A, Igarashi P: Intrarenal cells, not bone marrow-derived cells, are the major source for regeneration in postischemic kidney. *J Clin Invest* 115: 1756–1764, 2005

66. Dekel B, Shezen E, Even-Tov-Friedman S, Katchman H, Margalit R, Nagler A, Reisner Y: Transplantation of human hematopoietic stem cells into ischemic and growing kidneys suggests a role in vasculogenesis but not tubulogenesis. *Stem Cells* 24: 1185–1193, 2006

67. Togel F, Hu Z, Weiss K, Isaac J, Lange C, Westenfelder C: Administered mesenchymal stem cells protect against ischemic acute renal failure through differentiation-independent mechanisms. *Am J Physiol Renal Physiol* 289: F31–F42, 2005

Supplemental information for this article is available online at http://www.jasn.org/.